Surface Vibrational Modes of α-Quartz(0001) Probed by Sum-Frequency Spectroscopy

Wei-Tao Liu and Y. R. Shen*

Physics Department, University of California at Berkeley, Berkeley, California 94720, USA

(Received 26 March 2008; published 1 July 2008)

Infrared-visible sum-frequency spectroscopy was used to probe surface vibrations of α-quartz(0001) under ambient conditions. Two modes at 880 and 980 cm^{-1} were observed and identified as arising from Si-O-Si and Si-OH structures of the surface. Heat treatment and hydroxylation could convert Si-OH to Si-O-Si and vice versa. The technique is generally applicable to studies of surface phonons of other oxides, semiconductors, and insulators.

DOI: 10.1103/PhysRevLett.101.016101 PACS numbers: 68.35.Ja, 68.47.Gh, 78.68.+m

Surface phonons at a solid surface play an equivalent role as bulk phonons in the bulk of a solid. They are among the most important quantities characterizing a solid surface, and are intimately connected to a host of surface properties and phenomena [1]. Two well-established techniques are often used to study surface phonons: helium atom scattering (HAS) and electron energy loss spectroscopy (EELS). HAS is highly surface sensitive but restricted to the spectral range below 30 meV [2], and EELS spectra are usually dominated by the "macroscopic" Fuchs-Kliewer (FK) surface phonon-polaritons [3] appearing when $\mathrm{Re}(\varepsilon_B) = -1$, where $\varepsilon_B(\omega)$ is the bulk dielectric constant [4]. We are more interested in the "microscopic" surface phonons, which are more truly characteristic of surfaces [4]. Yet their experimental investigations are still rather limited [5] despite extensive theoretical studies [6]. In recent years, a novel fourth-order surface-specific nonlinear optical technique has been developed to probe such phonons [7,8]. In the process, Raman pumping is employed to excite the phonons and optical second harmonic generation to probe the excited phonons. However, the signal is weak, as expected from a fourth-order process, rendering measurements difficult [8]. More sensitive techniques are desired.

In this Letter, we report a study demonstrating that IR-visible sum-frequency spectroscopy (SFS) can be an effective tool to probe microscopic surface phonons and the related surface structures. Being a second-order process, SFS is surface-specific in media with inversion symmetry [9], and its signal strength is much stronger than fourth-order processes [10]. Even in media without inversion symmetry, it is possible to employ appropriate detection schemes to suppress sum-frequency (SF) contribution from the bulk and obtain SF spectra of the surface or interface [11]. FK phonons do not appear in the spectra because SF generation does not have resonance at $\mathrm{Re}(\varepsilon_B) = -1$ [9,10]. In our demonstrative study to be presented here, we used SFS to probe surface phonons of α-quartz(0001). Quartz was chosen because it is a representative and ubiquitous oxide. Oxide surfaces are relevant to many applications in fields ranging from chemistry and physics to environmental science and geoscience, but their structures have not been well studied [4,12]. Even for quartz surfaces, experimental information is limited and mostly acquired from atomic force microscopy (AFM), x-ray reflectivity, HAS, and low-energy electron diffraction (LEED) in ultrahigh vacuum [13–15]. On the other hand, a growing number of theoretical calculations on the microscopic structure of quartz surfaces have appeared in recent years [16–19], often using models with surfaces either completely hydroxylated or dehydroxylated. With SFS, we can now detect phonons originating from top surface monolayers of quartz in ambient conditions. The results should help elucidate the microscopic structure of quartz surfaces.

The basic theory for SFS was described elsewhere [9]. The SF signal, $S(\omega_{\mathrm{SF}})$, is given by

$$S(\omega_{\mathrm{SF}} = \omega_{\mathrm{vis}} + \omega_{\mathrm{IR}}) \propto |\chi^{(2)}_{\mathrm{eff}}|^2, \qquad \chi^{(2)}_{\mathrm{eff}} = [\hat{e}_{\mathrm{SF}} \cdot \vec{L}_{\mathrm{SF}}] \cdot (\vec{\chi}^{(2)}_S + i\vec{\chi}^{(2)}_B/\Delta k) : [\vec{L}_{\mathrm{vis}} \cdot \hat{e}_{\mathrm{vis}}][\vec{L}_{\mathrm{IR}} \cdot \hat{e}_{\mathrm{IR}}],$$
$$\vec{\chi}^{(2)}_S = \vec{\chi}^{(2)}_{S,\mathrm{NR}} + \sum_q \vec{A}^{(2)}_q/(\omega_{\mathrm{IR}} - \omega_q + i\Gamma_q), \qquad \vec{\chi}^{(2)}_B = \vec{\chi}^{(2)}_{B,\mathrm{NR}} + \sum_{q'} \vec{A}^{(2)}_{q'}/(\omega_{\mathrm{IR}} - \omega_{q'} + i\Gamma_{q'}), \tag{1}$$

where $\hat{e}_i$ and $\vec{L}_i$ are the unit polarization vector and transmission Fresnel coefficient at ω_i, Δk is the wave vector mismatch of the SF process, $\vec{\chi}^{(2)}_S$ and $\vec{\chi}^{(2)}_B$ are the surface and bulk nonlinear susceptibilities of the medium, $\vec{\chi}^{(2)}_{\mathrm{NR}}$ is the nonresonant contribution in $\vec{\chi}^{(2)}$, $\vec{A}^{(2)}_q$, ω_q, and Γ_q denote the amplitude, frequency, and damping coefficient of the qth resonance mode, respectively. Since surface and bulk generally belong to different symmetry groups, $\vec{\chi}^{(2)}_S$ and $\vec{\chi}^{(2)}_B$ can have distinctly different nonvanishing elements [10], allowing the separation of surface and bulk contributions to SF signals. While the bulk of α-quartz(0001) shows threefold symmetry (D_3) about the [0001] axis (also the surface normal), the surface should have sixfold symmetry (C_{6v}) because of unavoidable atomic steps and terraces. This was confirmed by LEED and HAS studies that displayed hexagonal diffraction pat-

terns [13,14]. In the crystal coordinates $(\hat{a}, \hat{b}, \hat{c})$, with $\hat{c}$ along [0001], $\hat{a}$ along the twofold axis and $\hat{a}$, $\hat{b} \perp \hat{c}$, the nonvanishing elements of $\vec{\chi}_S^{(2)}$ are $\chi_{S,ccc}^{(2)}$, $\chi_{S,aac}^{(2)} = \chi_{S,bbc}^{(2)}$, $\chi_{S,aca}^{(2)} = \chi_{S,bcb}^{(2)} \approx \chi_{S,caa}^{(2)} = \chi_{S,cbb}^{(2)}$, and the nonvanishing elements of $\vec{\chi}_B^{(2)}$ are $\chi_{B,aaa}^{(2)} = -\chi_{B,abb}^{(2)} = -\chi_{B,bba}^{(2)} = -\chi_{B,bab}^{(2)}$, $\chi_{B,abc}^{(2)} = -\chi_{B,bac}^{(2)}$, $\chi_{B,acb}^{(2)} = -\chi_{B,bca}^{(2)}$, and $\chi_{B,cab}^{(2)} = -\chi_{B,cba}^{(2)}$ [10]. Consider SFS with infrared and visible input beams incident on a sample with angles $\theta_{\rm vis} = 45°$ and $\theta_{\rm IR} = 57°$, respectively [see inset in Fig. 1(a)], and the incidence plane $(\hat{x} - \hat{z}$, with $\hat{Z} \parallel \hat{c})$ at an angle ϕ from the $\hat{a}$ axis. We have for input-output polarization combinations of *SSP* (denoting *S*-, *S*-, and *P*-polarized SF output, visible input, and IR input, respectively) and *PPP*,

$$\begin{aligned}
\chi_{SSP,\rm eff}^{(2)} &= L_{yy}(\omega_{\rm SF}) L_{yy}(\omega_{\rm vis}) [L_{zz}(\omega_{\rm IR}) \sin\theta_{\rm IR} \chi_{S,aac}^{(2)} \\
&\quad + L_{xx}(\omega_{\rm IR}) \cos\theta_{\rm IR} i \chi_{B,aaa}^{(2)} \cos 3\phi / \Delta k] \\
\chi_{PPP,\rm eff}^{(2)} &\approx -L_{xx}(\omega_{\rm SF}) L_{xx}(\omega_{\rm vis}) L_{zz}(\omega_{\rm IR}) \\
&\quad \times \cos\theta_{\rm SF} \cos\theta_{\rm vis} \sin\theta_{\rm IR} \chi_{S,aac}^{(2)} \\
&\quad + L_{zz}(\omega_{\rm SF}) L_{zz}(\omega_{\rm vis}) L_{zz}(\omega_{\rm IR}) \\
&\quad \times \sin\theta_{\rm SF} \sin\theta_{\rm vis} \sin\theta_{\rm IR} \chi_{S,ccc}^{(2)} \\
&\quad + L_{xx}(\omega_{\rm SF}) L_{xx}(\omega_{\rm vis}) L_{xx}(\omega_{\rm IR}) \\
&\quad \times \cos\theta_{\rm SF} \cos\theta_{\rm vis} \cos\theta_{\rm IR} i \chi_{B,aaa}^{(2)} \cos 3\phi / \Delta k.
\end{aligned} \tag{2}$$

It is readily seen that if we set ϕ to make $\cos 3\phi$ vanish, then SFS only depends on $\vec{\chi}_S^{(2)}$.

Our experimental arrangement of SFS is similar to that described in Ref. [9] and depicted in the inset of Fig. 1(a). Briefly, the IR input pulses tunable between 9 and 13 μm with $\sim$30 μJ/pulse and the visible input pulses fixed at 0.532 μm with $\sim$500 μJ/pulse were both derived from a picosecond Nd:YAG laser or optical parametric system, each with 20 ps pulse length and 20 Hz repetition rate. They were directed to overlap at the sample surface and the reflected SF signal was recorded. The SF signal from a sample was normalized against that from a GaAs(110) wafer. The α-quartz(0001) samples of 5 mm thick and $\sim$0.5 nm rms roughness were purchased from Princeton Scientific Corp. The surfaces are cleaned and hydroxylated following the procedure described in Ref. [11]. Their SF spectra exhibited no trace of C-H stretch vibrations, indicating negligible hydrocarbon surface contamination. For comparison, amorphous silica slabs were also studied in the experiment. They were treated with the same procedure for quartz. All measurements were carried out under ambient atmosphere and room temperature.

The SF-active bulk phonons of α-quartz appear at 795, 1064, and 1160 cm^{-1} in the IR range we probed [20,21]. With these modes suppressed, we could observe resonant bands in the 850–1050 cm^{-1} range where bulk resonances are absent [21]. Figure 1(a) displays the *SSP*-SF spectra in the 850–1150 cm^{-1} range obtained from α-quartz(0001) at different ϕ. The 1064 cm^{-1} bulk mode is strongly suppressed when ϕ goes from 31.8° to 30° (residual trace of the peak is due to nonideal alignment), while resonances within 850–1050 cm^{-1} show little change with respect to ϕ. This allows us to identify peaks at 980 and 880 cm^{-1}, with $\Gamma_q = 23$ and 31 cm^{-1}, respectively, as surface modes. To support the identification, we took the SSP spectrum of α-quartz(0001) perturbed by monolayer coverage of octadecyltrichlorosilane (OTS) [22]. As shown in Fig. 1(b), the peak at 980 cm^{-1} is almost quenched and the one at 880 cm^{-1} also reduced, indicating that both are indeed surface originated.

To assign the observed resonances, we note that the cleaned quartz surface was hydrophilic and should be at least partially hydroxylated. The OTS monolayer is chemically bonded to the quartz surface by replacing H at Si-OH sites [22], and this would also happen on amorphous silica. For comparison, therefore, we took the SSP spectra of silica, presented in Fig. 1(c). Only a peak at $\sim$970 cm^{-1} appears in the spectrum of the bare silica surface, which is greatly reduced with the OTS coverage. Thus we can assign the 980 cm^{-1} mode of quartz and the 970 cm^{-1} mode of silica to Si-OH stretch vibration, as both are suppressed when OTS replaces H on the surfaces. This assignment is supported by spectroscopic studies of high-

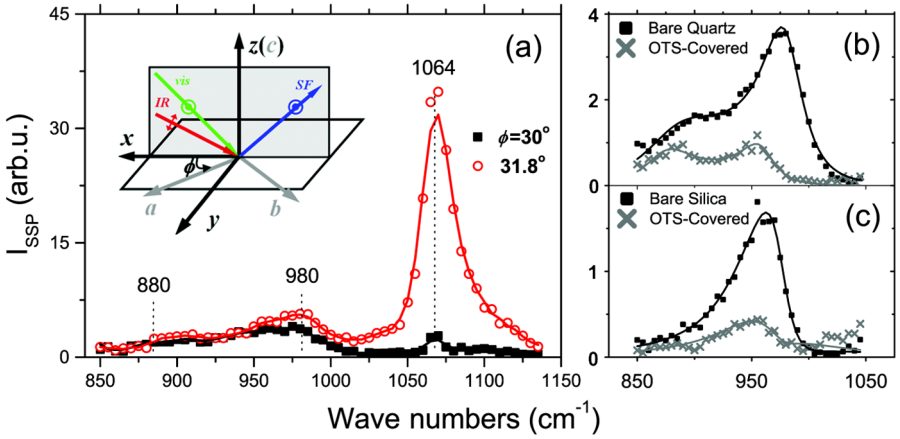

FIG. 1 (color online). (a) *SSP*-SF spectra of α-quartz(0001) taken at $\phi =$ 30° and 31.8° (curves are guides to eyes). (b),(c) *SSP*-SF spectra at $\phi =$ 30° of, respectively, bare (solid squares) and OTS-covered (crosses) α-quartz(0001) and bare (solid squares) and OTS-covered (crosses) amorphous silica; solid curves are fits using Eq. (1). The inset describes the beam geometry.

surface-area silica particles [23,24]. The 880 cm^{-1} mode, which is less perturbed by OTS and does not exist on amorphous silica, must come from the unhydrated, ordered Si-O-Si structures of the (0001) crystalline surface. Similar IR bands at ~890 and 910 cm^{-1} were observed in silica particles upon dehydroxylation [25].

To further confirm our assignment, we attempted heating to remove H from the hydroxylated sample surfaces ($2Si\text{-}OH \rightarrow Si\text{-}O\text{-}Si + H_2O$) [23,25], and expected to see a drop of the Si-OH mode and an increase of the Si-O-Si mode. We baked the freshly cleaned quartz at 100 °C for 30 min, and then cooled it down to room temperature in an evacuated desiccator. The heat-treated surface remained stable for at least 6 h, as judged by its *SSP* and *PPP* spectra presented in Fig. 2(b) (solid squares). In comparison with the freshly cleaned surfaces of α-quartz(0001) [Fig. 2(a)], the 980 cm^{-1} peak clearly drops and the 880 cm^{-1} mode increases, indicating conversion of surface groups from Si-OH to Si-O-Si. We expect the dehydroxylation process to be reversible. Indeed, after subjecting the sample to hydroxylation, the spectra fully recovered to those of the freshly cleaned one (open circles).

The surface mode at 880 cm^{-1} is adjacent to the bulk phonon at 795 cm^{-1}, and the large shift indicates it comes from a distorted or reconstructed Si-O-Si surface structure. We notice that the *ab initio* calculation of unhydrated α-quartz(0001) shows reconstructed surface groups with Si-O bond length and O-Si-O bond angle close to the bulk values, but a Si-O-Si bond angle of ~130°, different from the bulk value of 143.7° [19]. The 795 cm^{-1} phonon is due to symmetric stretches of bulk Si-O-Si bonds [26]. If we adopt the force constants for stretching and bending vibrations of Si-O-Si in α-quartz (4.3×10^5 and 0.4×10^5 dyn/cm, respectively [23]), then the reconstructed Si-O-Si structure should have its symmetric stretching frequency scaled from 795 to ~870 cm^{-1} [27], close to the observed frequency at 880 cm^{-1}. This provides support to the picture of surface reconstruction with strained Si-O-Si groups, but further theoretical investigation of the surface structure is still needed, particularly for those partially covered with H.

The reconstruction also affects the orientation of Si-OH groups on quartz. The Si-OH bond orientation can be obtained from the relative strengths of the 980 cm^{-1} mode in *SSP* and *PPP* spectra following the analytical procedure described in Ref. [28]. Briefly, we first deduce $A^{(2)}_{q,ijk}$ for the mode by fitting the spectra using Eqs. (1) and (2) with Fresnel coefficients calculated from known refractive indices [29] and then obtain the polar orientation of the bond from the ratio of $|A^{(2)}_{q,aac}/A^{(2)}_{q,ccc}|$ using bond polarizability parameters given in Ref. [30]. We found the average Si-OH orientation from the surface normal to be $\leq 30°$, which is smaller than the two Si-O bond orientations of 47° and 67° if the surface is bulk-terminated. Since the neighboring distance between Si on a bulk-terminated (0001) surface is larger than twice the Si-O bond length, the formation of Si-O-Si at the surface will distort the adjacent surface structure, resulting in tilting of neighboring Si-OH bonds more toward the surface normal. Figure 2(d) shows a schematic of the structure of α-quartz(0001) composed of Si-OH and Si-O-Si.

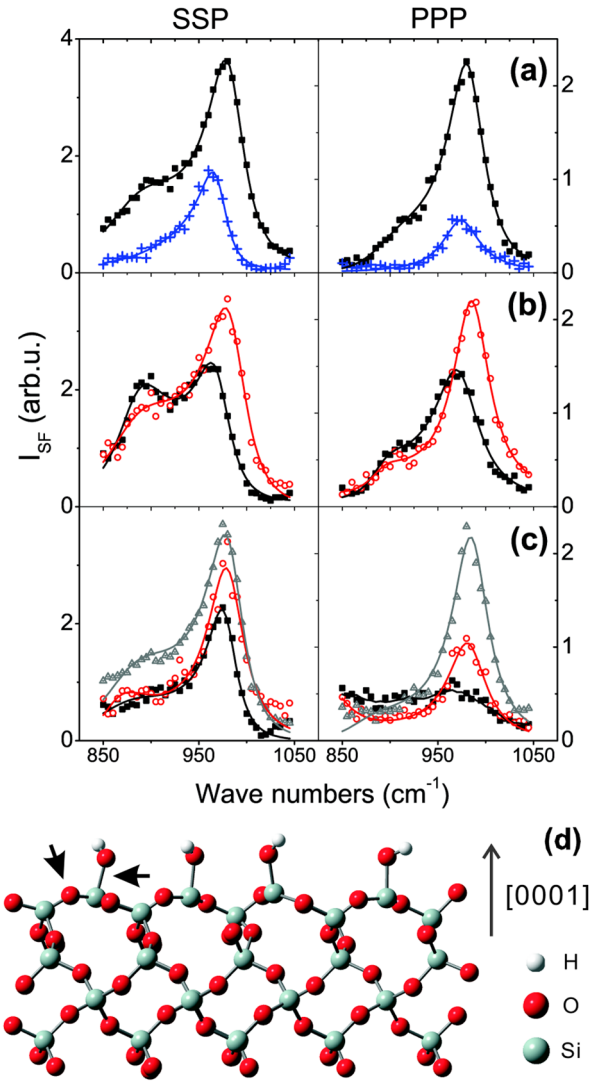

FIG. 2 (color online). *SSP*- and *PPP*-SF spectra of (a) freshly cleaned α-quartz(0001) (solid squares) and amorphous silica (crosses), (b) α-quartz(0001) after being baked at 100 °C (solid squares) and rehydroxylated (open circles), and (c) α-quartz(0001) after being baked at 500 °C (solid squares), rehydroxylated (open circles), and boiled in distilled water (open triangles). Solid curves are fits using Eq. (1). (d) Possible structure of α-quartz(0001) composed of both Si-OH and Si-O-Si (indicated by arrows).

While heating dehydroxylates the quartz surface, it may cause irreversible surface structural changes if the baking temperature is too high. Presented in Fig. 2(c) are *SSP* and *PPP* spectra of α-quartz(0001) taken at room temperature after being baked at 500 °C for 30 min (solid squares). The 980 cm^{-1} peak drops in both spectra, but more precipitously in *PPP*, indicating broad spread of Si-OH bond orientations. The 880 cm^{-1} peak significantly drops in

SSP and broadens in both spectra, suggesting disruption of the ordered Si-O-Si structure. The usual hydroxylation procedure recovers partially the 980 cm^{-1} peak, but not the 880 cm^{-1} mode (open circles). Recent AFM study denoted that bathing in water at 127 °C could remove amorphous or damaged layers on low-index quartz surfaces [15]. We found indeed that boiling the 500 °C-heat-treated sample in distilled water for ~12 h recovered its SF spectra to those of the freshly cleaned sample (open triangles). Surface damage also occurred at lower baking temperatures to a lesser extent. The observation correlates well with the room-temperature LEED study on α-quartz(0001) that showed a deteriorated LEED pattern after the sample being pretreated at ~500 °C in air [13]. That surface structural change happens at a temperature much lower than any bulk phase transition is probably common for many oxides, for example, α-alumina [31]. This could have important consequences in applications involving oxide surfaces.

In summary, using α-quartz(0001) as a representative system, we have demonstrated that SFS is a viable spectroscopic tool to probe surface phonons and structures of oxides. We identified two surface modes, one at 980 cm^{-1} from Si-OH stretch vibration and the other at 880 cm^{-1} from reconstructed Si-O-Si surface structures. Results indicate that under ambient conditions a freshly cleaned surface is composed of a reconstructed Si-O-Si network partially covered by Si-OH groups. Heating dehydroxylates Si-OH and converts them to Si-O-Si, but baking at high temperature causes severe surface structural distortion that can only be removed by aggressive rehydroxylation.

This work was supported by the Director, Office of Science, Office of Basic Energy Sciences, Materials Sciences and Engineering Division, of the U.S. Department of Energy under Contract No. DE-AC03-76SF00098.

*yrshen@calmail.berkeley.edu

[1] *Surface Phonons*, Springer Series in Surface Science Vol. 21, edited by W. Kress and F. W. de Wette (Springer, Berlin, 1990).
[2] *Helium Atom Scattering from Surfaces*, Springer Series in Surface Science Vol. 27, edited by E. Hulpke (Springer, Berlin, 1992).
[3] R. Fuchs and K. L. Kliewer, Phys. Rev. **140**, A2076 (1965).
[4] V. E. Heinrich and P. A. Cox, *The Surface Science of Metal Oxides* (Cambridge University Press, Cambridge, England, 1994).
[5] See, for example, a few cases of EELS study quoted in Ref. [4] and a case of resonant Raman scattering study by K. Hinrichs, A. Schierhorn, P. Haier, N. Esser, W. Richter, and J. Sahm, Phys. Rev. Lett. **79**, 1094 (1997).
[6] See, for example, V. Shpakov, A. Gotte, M. Baudin, T. Woo, and K. Hermansson, Phys. Rev. B **72**, 195427 (2005); T. E. Karakasidis, Surf. Sci. **600**, 4089 (2006).
[7] Y. M. Chang, L. Xu, and H. W. K. Tom, Phys. Rev. Lett. **78**, 4649 (1997); Phys. Rev. B **59**, 12220 (1999).
[8] S. Fujiyoshi, T.-A. Ishibashi, and H. Onishi, J. Phys. Chem. B **109**, 8557 (2005); T. Nomoto and H. Onishi, Phys. Chem. Chem. Phys. **9**, 5515 (2007).
[9] Y. R. Shen, Proc. Natl. Acad. Sci. U.S.A. **93**, 12104 (1996).
[10] Y. R. Shen, *The Principles of Nonlinear Optics* (Wiley, New York, 1984).
[11] V. Ostroverkhov, G. A. Waychunas, and Y. R. Shen, Chem. Phys. Lett. **386**, 144 (2004); Phys. Rev. Lett. **94**, 046102 (2005).
[12] C. Noguera, *Physics and Chemistry at Oxide Surfaces* (Cambridge University Press, Cambridge, England, 1996).
[13] I. Janossy, Surf. Sci. **25**, 647 (1971); F. Bart and M. Gautier, Surf. Sci. **311**, L671 (1994); M. L. Schlegel, K. L. Nagy, P. Fenter, and N. C. Sturchio, Geochim. Cosmochim. Acta **66**, 3037 (2002).
[14] W. Steurer, A. Apfolter, M. Koch, T. Scarlat, E. Sondergard, W. E. Ernst, and B. Holst, Surf. Sci. **601**, 4407 (2007).
[15] A. J. Gratz, S. Manne, and P. K. Hansma, Science **251**, 1343 (1991); M. Kawasaki, K. Onuma, and I. Sunagawa, J. Cryst. Growth **258**, 188 (2003); S. V. Yanina, K. M. Rosso, and P. Meakin, Geochim. Cosmochim. Acta **70**, 1113 (2006).
[16] N. H. de Leeuw, F. M. Higgins, and S. C. Parker, J. Phys. Chem. B **103**, 1270 (1999).
[17] G. M. Rignanese, A. De Vita, J. C. Charlier, X. Gonze, and R. Car, Phys. Rev. B **61**, 13 250 (2000); G. M. Rignanese, J.-C. Charlier, and X. Gonze, Phys. Chem. Chem. Phys. **6**, 1920 (2004).
[18] V. V. Murashov, J. Phys. Chem. B **109**, 4144 (2005).
[19] T. P. M. Goumans, A. Wander, W. A. Brown, and C. R. A. Catlow, Phys. Chem. Chem. Phys. **9**, 2146 (2007).
[20] Wei-Tao Liu and Y. R. Shen, Phys. Rev. B (to be published).
[21] X. Gonze, D. C. Allan, and M. P. Teter, Phys. Rev. Lett. **68**, 3603 (1992).
[22] J. Sagiv, J. Am. Chem. Soc. **102**, 92 (1980).
[23] R. L. White and A. Nair, Appl. Spectrosc. **44**, 69 (1990).
[24] D. P. Zarubin, J. Non-Cryst. Solids **286**, 80 (2001); C. Carteret, Spectrochim. Acta, Part A **64**, 670 (2006).
[25] A. Grabbe, T. A. Michalske, and W. L. Smith, J. Phys. Chem. **99**, 4648 (1995); D. Ceresoli, M. Bernasconi, S. Iarlori, M. Parrinello, and E. Tosatti, Phys. Rev. Lett. **84**, 3887 (2000).
[26] *The Infrared Spectra of Minerals*, edited by V. C. Farmer (Mineralogical Society, London, 1974), Chap. 16.
[27] G. Herzberg, *Infrared and Raman Spectra of Polyatomic Molecules* (Van Nostrand, New York, 1945), p. 169.
[28] X. Wei, Ph.D. thesis, University of California at Berkeley, 2000; X. Wei, P. B. Miranda, C. Zhang, and Y. R. Shen, Phys. Rev. B **66**, 085401 (2002).
[29] *Handbook of Optical Constants of Solids*, edited by E. Palik (Elsevier, New York, 1998).
[30] P. Umari, A. Pasquarello, and A. A. DalCorso, Phys. Rev. B **63**, 094305 (2001); K. Smirnov, D. Bougeard, and P. Tandon, J. Phys. Chem. A **110**, 4516 (2006).
[31] T. N. Rhodin, B. G. Frederick, and G. Apai, Surf. Sci. **287/288**, 638 (1993).